Acta Zoologica (Stockholm) **90**: 132–141 (April 2009) doi: 10.1111/j.1463-6395.2008.00338.x

Organization and mode of secretion of the granular prismatic microstructure of *Entodesma navicula* (Bivalvia: Mollusca)

Elizabeth M. Harper,[1] Antonio G. Checa[2] and Alejandro B. Rodríguez-Navarro[3]

[1]Department of Earth Sciences, Cambridge University, Downing Street, Cambridge, CB2 3EQ, United Kingdom; [2]Departamento de Estratigrafía y Palaeontología; [3]Departamento de Mineralogía y Petrología, Facultad de Ciencias, Universidad de Granada, E-18171 Granada, Spain

Accepted for publication: 13 May 2008

Abstract

Harper, E. M., Checa, A. G. and Rodríguez-Navarro, A. B. 2009. Organization and mode of secretion of the granular prismatic microstructure of *Entodesma navicula* (Bivalvia: Mollusca). — *Acta Zoologica* (Stockholm) **90**: 132–141.

The term homogeneous has been applied to molluscan microstructures that lack a readily discernible microstructure and as a result, it has become rather a 'dustbin' term, covering a multitude of unrelated finely crystalline textures. Here we investigate in detail the outer 'homogeneous' layer of the lyonsiid bivalve *Entodesma navicula*. The apparently equigranular crystals (up to 10 μm) are, in fact, short prisms which grow in a dense organic matrix with their *c*-axes and fibre axes coincident, perpendicular to the growth surface. These prisms are distinct from the aragonitic prisms grown by other bivalves in both their morphology and their mode of growth and so we propose the term *granular prismatic* microstructure. The organic content of granular prisms (7.4%) is the highest yet recorded for any molluscan microstructure and it is apparent that the short prisms have grown within a gel-filled space. Although this high organic content is likely to make the microstructure metabolically expensive to produce, it has the benefit of making the valves very flexible. This may be advantageous in the intertidal zone inhabited by *E. navicula* by allowing a tight seal between the valves.

Elizabeth M. Harper, Department of Earth Sciences, Cambridge University, Downing Street, Cambridge, CB2 3EQ, United Kingdom.
E-mail: emh21@cam.ac.uk

Introduction

Molluscan shell is a composite material with crystals of calcium carbonate (as either aragonite or calcite) dispersed within an organic matrix. A number of possible microstructures have been recognized which fall into the broad categories of aragonitic prisms, nacre, homogeneous, crossed-lamellar and complex crossed-lamellar structures and calcitic prisms or foliae (Bøggild 1930; Taylor *et al.* 1969, 1973; Carter *et al.* 1985). All shells contain at least two of these different microstructural types, typically arranged in discrete layers. The identity of the microstructural layers and their distribution within the shell of particular taxa has been found to have both phylogenetic and adaptive significance (Taylor *et al.* 1969, 1973; Carter 1980). Additionally, the study of shell microstructures is potentially of great interest to the field of biomechanics and biomedicine. Nacre is stronger in compression and bending than vertebrate bone (Currey 1970; Taylor and Layman 1972) and Lin *et al.* (2008) have shown that nacre is 3000 times stronger than inorganic aragonite. Additionally the calcite prismatic layer of *Ostrea edulis* is exceptionally flexible (Zhou and Checa, unpublished results 2007). Nacre is the only molluscan microstructure to have been tested for clinical–medical applications (Camprase *et al.* 1990; Atlan *et al.* 1997) but it is clear that others may follow.

Many molluscan microstructures have been studied in detail and are highly ordered structures (e.g. Checa and Rodríguez-Navarro 2001, 2005). However, aragonitic homogeneous structures are less well known. The term was first used by Bøggild (1930) and adopted by subsequent authors (e.g. Oberling 1964; Taylor *et al.* 1969, 1973) to apply to rather non-descript fine-grained structures. As noted by Taylor *et al.* (1969; p. 51), it is a 'term of convenience' used for a crystalline texture that is too fine to discern easily a recognizable pattern, a particular problem when low

resolution is available. A subsequent study by Carter (1980) sought to subdivide the homogeneous shell microstructure into a fine homogeneous *sensu stricto* with crystals less than 5 μm in diameter and a more granular homogeneous structure where the crystals were larger. However, this definition is difficult to apply because it is clear that in many samples both are present (see Carter 1980; Appendix 2B fig. 47).

Homogeneous microstructure has been reported for a range of bivalve taxa including the nuculanoids, solemyoids and various heterodont groups such that it is apparent that its possession does not define a monophyletic group (i.e. the microstructure has not appeared as a single innovation). Taylor (1973; p. 522) suggested that homogeneous microstructures resulted from the breakdown of other recognizable microstructures and hypothesized that further study is likely to reveal different types. These comments have proved accurate in the case of the heterodont bivalve *Arctica islandica* in which detailed study of the homogeneous layer revealed that it is in fact a miniaturized crossed-lamellar microstructure (Ropes *et al.* 1983). Elsewhere among the heterodonts, within the anomalodesmatans, there appear to be at least two different styles of homogeneous microstructure (Harper *et al.* 2006; fig. 6): a granular structure in some members of the family Lyonsiidae, described by Prezant (1981a), and a much finer structure seen in the carnivorous cuspidariids [which appears to show vestiges of a crossed-lamellar like structure, as indeed do some thraciid bivalves (unpublished observations)].

In this paper we study the granular homogeneous microstructure found in the lyonsiid bivalve *Entodesma* in greater detail. Its general appearance is one of more or less equant grains up to 10 μm across with no obvious orientation (Fig. 1). Prezant (1981a) described these granules as being made of spherules and suggested that they might be derived from aragonite prisms. He suggested that this would be a cheap and rapidly laid down shell microstructure. Our preliminary studies of this shell microstructure revealed, however, that it was rather unusual in a number of respects and our aim has been to use a battery of modern techniques to provide further characterization of the microstructure, and to consider its genesis and possible functional significance.

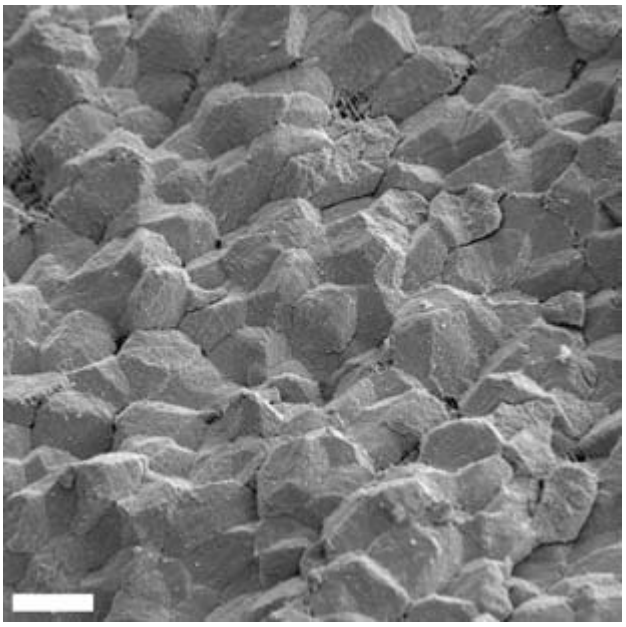

Fig. 1—Scanning electron micrograph of the 'homogeneous' layer of *Entodesma navicula*. Fractured section through the valve. Scale bar = 10 μm.

Lysonsiid bivalves

The anomalodesmatan family Lyonsiidae is widely considered to comprise three extant genera: *Lyonsia*, *Entodesma* and *Mytilimeria* (Prezant 1981b). Species of *Lyonsia*, the genus with the longest known evolutionary history (first appearing in the Eocene) and the broadest geographical distribution, are shallow burrowers and show typical anomalodesmatan shell structure of a very thin (< 5 μm) external layer of aragonite prisms and thicker internal layers of sheet and lenticular nacre (Carpenter 1847; Prezant 1981a). The other two genera, *Entodesma* and *Mytilimeria*, have a much more recent first appearance in the fossil record and are restricted to the Pacific and the Gulf of Mexico. The general consensus is that *Entodesma* and *Mytilimeria* are derived from a *Lyonsia*-like ancestor (Yonge 1952; Prezant 1981b,c; Harper *et al.* 2006). Both derived genera have more sedentary, nestling life habits, the latter in intimate association with ascidians (Yonge 1952). Representatives of both genera have nacreous inner shells but the outer shell layer of some species of *Entodesma* (*E. navicula*, *E. truncatissima* and *E. cuneata*) and the sole species of *Mytilimeria*, *M. nutalli*, have been described as homogeneous [albeit only a very thin layer in the latter taxon (Prezant 1981a)]. In this study we specifically investigate this homogeneous layer in *E. navicula* (Adams & Reeve 1850) in which it is particularly well developed.

Entodesma navicula (Fig. 2) occurs in an arc around the northern Pacific from California, through the western coast of the USA and Canada, Alaska, the Bering Sea and westwards into the Kurile Islands and northern Japan (Coan *et al.* 2000). Unfortunately in key papers describing the biology and functional morphology of this species (e.g. Yonge 1952; Morgan and Allen 1976; Morris *et al.* 1980; Prezant 1981a,b,c; Morton 1987) it is known by its junior synonym *Entodesma saxicola* (Baird 1863), a name which had been applied to North American specimens that show no morphological difference from those bearing the older name from Japan (Coan, personal communication). It has a relatively large (up to 150 mm in length), slightly inequivalve, heteromyarian shell, which is frequently highly distorted because of its habit of permanent byssate attachment between rocks and in crevices (Yonge 1952; Morris *et al.*

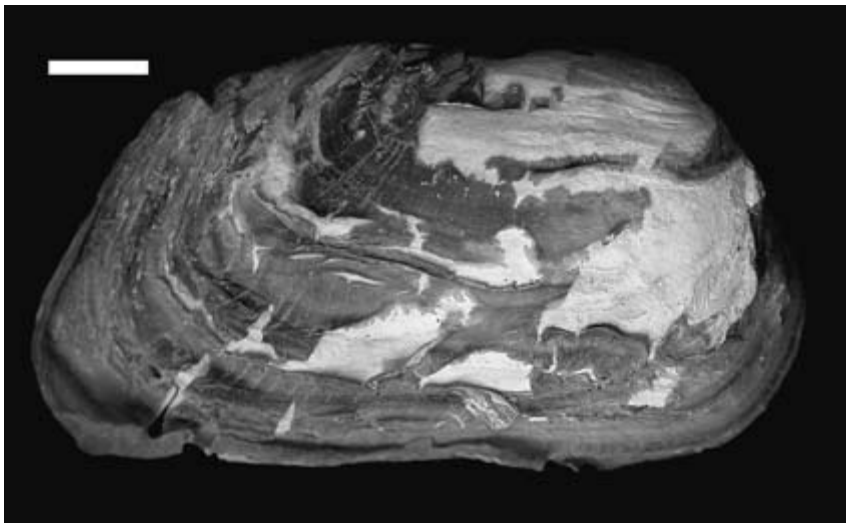

Fig. 2—External view of the right valve of *Entodesma navicula* collected from Hokkaido in Japan. Scale bar = 10 mm.

1980). It has been reported from the intertidal zone to depths of 60 m (Coan *et al.* 2000).

Materials and Methods

Individuals of *E. navicula* were obtained through the kindness of Dr Roland Anderson (Seattle Aquarium). They were collected from Mushroom Rock, Cape Flattery, WA, USA from a water depth of 13 m. They were preserved in 100% ethanol and the soft parts were used in the molecular study conducted by Dreyer *et al.* (2003). Subsequently, the shell material was air-dried and kept pending this study. Comparative material of two other thin-shelled species, *Entodesma beana* a sponge associate from the Florida Keys and *Entodesma pictum* from Bahia Angeles, Mexico were obtained from the Field Museum (Chicago, IL) and the Santa Barbara Museum (Santa Barbara, CA), respectively.

Optical and electron microscopy

Standard petrological thin sections were made through the valves of *E. navicula* along the line of maximum shell growth and were observed using optical microscopy. Material for scanning electron microscopy (SEM) was prepared to allow the examination of fractured surfaces through the thickness of the shell and of the internal surfaces of the valve. In most cases there was no further preparation of the material apart from ultrasonic cleaning and air drying. However, in a few cases, we removed either the organic or the mineral matter using 20% NaClO for 2–10 min or 2–4% ethylenediaminetetraacetic acid (EDTA) for 20 min, respectively, at room temperature. Samples were either coated with carbon for field emission SEM observation (Gemini 1530, Leo, Germany), or gold-coated for inspection by SEM (Jeol 820). Fractures through the shells of *E. beana* and *E. pictum* were also examined for comparison.

Samples for transmission electron microscopy (TEM) were prepared either intact or completely decalcified with 2% EDTA over several days. They were sectioned with an ultramicrotome LEICA Ultracut R and prepared following standard procedures. Intact samples were observed in a high-resolution TEM Philips CM20 machine, whereas decalcified samples were observed in a TEM Zeiss EM 10C.

Thermogravimetry

The organic content of the homogeneous microstructure was investigated by thermogravimetry. Two samples, of approximately 50 mg, were taken from the isolated shell microstructure (from the same shell) and powdered before analysis using a thermogravimetric analyser (SHIMADZU TGA-50H) over a temperature range from 25 to 950 °C. Percentage weight losses at < 165°, 165–275°, 275–600° and > 600 °C were calculated.

X-ray diffraction

The three-dimensional orientation of the crystals that make up the homogeneous layer of *E. navicula* was determined using an X-ray single diffractometer equipped with an area detector (D8 SMART APEX, Bruker, Germany). Shell samples were measured by reflection using Mo Kα radiation, a pin-hole collimator of 0.5 mm diameter and an exposure time of 20 s per frame (512 × 512 pixels). A set of frames (two-dimensional diffraction patterns) was registered while rotating the sample around ψ angle (a frame every 5° and 36 frames in total). From this set of frames, the pole figure densities for some of the strongest aragonite reflections (111, 002, 012, 112, 220) were calculated and displayed in stereographic projection using XRD2DSCAN software (Rodríguez-Navarro 2007). The X-ray analyses were conducted for both the external (after removing the periostracum) and internal

surface of the shell (close to the boundary with nacre) and for vertical fractures through the valve.

Results

Our observations confirm the basic arrangement of shell microstructures described for *E. navicula* and *E. beana* by Prezant (1981b). The *E. navicula* has a thick persistent periostracum but lacks the outer prismatic layer typical of most other anomalodesmatans and is composed, instead, of a granular 'homogeneous layer', with nacre inside. In the case of both *E. beana* and *E. pictum* (the microstructure of which has not previously been reported) were found to have thinner (10 μm or less) periostraca, and to lack a homogeneous layer comparable to that seen in *E. navicula.* Instead, in both taxa the outermost shell layer was prismatic and approximately 10 μm thick. The form of these prisms was not studied in detail but they did not resemble the spherulitic growths seen in neotigoniids and unionids (see Discussion).

Detailed observations for Entodesma navicula

The external surface of the shell is covered by a thick layer of brown periostracum that extends ventrally past the calcareous part of the shell. The layer is frequently wrinkled, often with radial pleating, and there is a tendency in air-dried specimens from museum collections for the periostracum to part from the shell (see Fig. 2), and often for the shell itself to fragment. The outer shell is composed of a thick (up to 2 mm) layer of granular 'homogeneous' structure (described in detail below), with an inner layer of nacre. The inner nacre layer extends close to the ventral edge of the valve, albeit thinning considerably towards the margins. The two shell layers are readily discernible even with the naked eye; the homogeneous layer appearing orange in colour, whereas the nacre is a pearly grey. The boundary between the two shell layers does not coincide with the disjunct pallial line, which is located deeper within the nacreous layer.

Observations of sections through shell layers

The periostracum is thick (at least 100 μm). Two layers are present; a thinner (approximately 3 μm) outer layer and a much thicker inner layer (Fig. 3A). The transition between the lower boundary of the periostracum and the calcareous shell is not sharp. Instead crystals appear growing *within* the lower periostracum and thin layers of periostracum (10–20 μm) are encountered deep within the 'homogeneous' layer (Fig. 4A). A fine-scale internal banding is evident within periostracum using TEM (Fig. 3B) with the spacing between these bands irregular, ranging from tens of nanometers to 100 nm.

There is no columnar prismatic layer growing directly internal to the periostracum, as there is in *E. beana* and *E. pictum*. Instead, the layer immediately inside the periostracum is composed of tightly packed irregular polyhedral grains of aragonite. These crystals vary in size but are mostly 3–10 μm across (Fig. 4B). Growth lines are evident within these crystals and may be traced across neighbouring crystals. The grains themselves are anhedral in general, except along some growth bands where there is some free space between them and in these instances crystal faces develop (Fig. 4C). The crystal shapes developed in this way are short prisms composed of parallel fibres with arrow point endings (Fig. 4C,D,J). In most cases these short prismatic crystals are arranged perpendicular, or nearly so, to the internal growth lines but in some exceptional areas, prisms grow in a disorientated fashion and in these instances the crystals are fibrous and 'skeletal' (Fig. 4D,J). Where the section passes through the ventral-most portion of the valve where there is no underlying nacreous layer, the growth surface is not smooth (as is the case in typical bivalves) but instead shows a rough topography with individual crystals protruding by different amounts (Fig. 4I).

It is evident from decalcified sections and TEM that there is a large amount of organic material associated with the granular crystals (Figs 3C,D and 4F). Each crystal is surrounded by an organic rim of variable thickness and the crystals themselves display internal membranes.

Towards the transition to the inner shell layer of nacre the morphology of the 'granular' crystals changes, becoming more elongate towards the interior surface of the shell (Fig. 4G), and so more reminiscent of microstructures typically classified as prismatic aragonite. The internal banding remains present and the transition between these prisms and the nacre is sharp. Observation with TEM shows also that the transition is marked by the appearance of dense interlamellar layers (Fig. 3F)

Observations of growth surfaces

Examination of the growth surfaces reveals very short prisms growing in a dense organic material which occurs either as sheets or as more substantial masses (Fig. 4H,I,K,L). On some surfaces it is evident that there are marked differences between the density of crystals over small distances (Fig. 4H). Observations of a single growth surface reveal that, over a small area, crystals show a range of sizes (1–10 μm) and project from the surface by different amounts (Fig. 4E,K,L). These crystals have a tendency to develop a pseudohexagonal outline with evidence from the 120° fracture pattern (Fig. 4K) and the elongation of the transverse section of fibres (Fig. 4J); the crystals are twinned along the {110} planes. Towards the nacre, the crystals on the growth surfaces become so closely packed as to form a pavement.

Thermogravimetry

The two analysed samples showed four consecutive losses of weight with means of 0.84% (100–165 °C), 1.68%

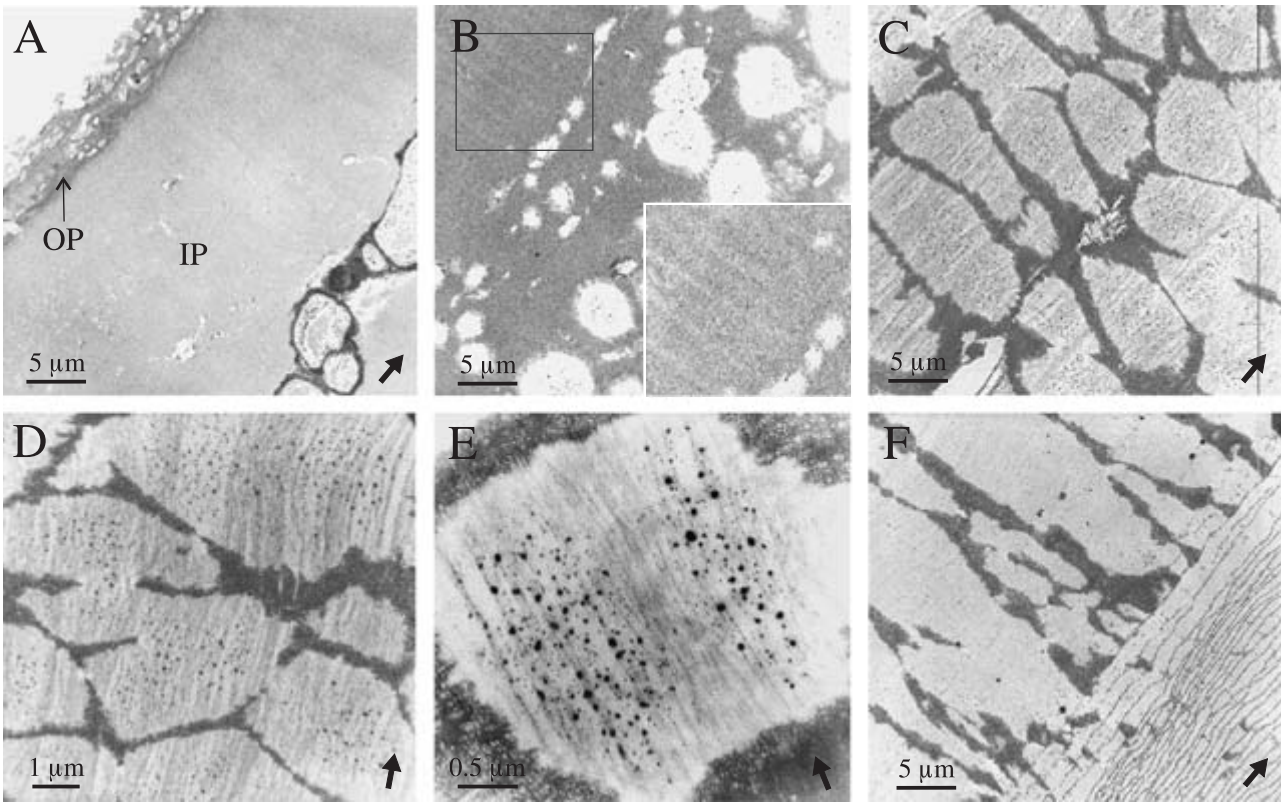

Fig. 3—Transmission electron micrographs of completely decalcified samples of the 'homogeneous' microstructural layer of *Entodesma navicula*. All sections are longitudinal and perpendicular to the shell surfaces. —**A**. View of the thin outer (OP) and the thick inner (IP) periostracum. —**B**. Gradual transition from the inner periostracum to the homogeneous layer. The inset is a magnification of the rectangle and shows the fine horizontal banding internal to the periostracum. —**C**. Interior of the homogeneous layer showing the same banding in the interior of the decalcified granules. —**D**. Detail of fine bands passing across the boundaries between grains. —**E**. Detail of the interior of a grain showing the nanometric spacing of bands. —**F**. Section at the boundary between the 'prismatic' part of the granular layer and the underlying nacreous layer; the boundary is marked by the disappearance of the thick intergranular organic membranes and the development of the thin interlamellar membranes of nacre. Arrows indicate the growth direction of the margin.

(165–275 °C), 5.74% (275–600 °C) and 38.48% (> 600 °C). The first loss was attributed to complete loss of water and the fourth to the thermal decomposition of the $CaCO_3$ releasing CO_2. The second and third are losses were the result of combustion of the organic matrix, as inter- and intracrystalline matrix, respectively, within the shell and imply a total organic matter content of approximately 7.4%.

X-ray analysis

The pole figures obtained by X-ray analysis for the 'homogeneous' layer are shown in Fig. 5. Each pole figure displays the intensity variation of a given hkl reflection as a function of the sample orientation. From these plots, the three-dimensional orientation of associated {hkl} crystal faces can be observed and the preferential orientation of crystals making the sample characterized. The 002 pole figures obtained indicate that grains display a general orientation with their *c*-axis perpendicular to the outer and inner layer surface. By contrast the pole figures for the 211, 220, 132 and, particularly, 111 demonstrate that the crystals have their *a*-axis and *b*-axis mutually disoriented, rotated around the *c*-axis. The implication of these findings is that the microstructure has a fibre texture, where the *c*-axis and fibre axis are coincident.

Discussion

The 'homogeneous' microstructure seen in the lyonsiid bivalves, and exemplified by *E. navicula* herein, is clearly distinct from other molluscan microstructures that have been described as homogeneous, e.g. *A. islandica*. We have been able to extend the work of Prezant (1981a) to further characterize the organization of the microstructure and to use this information to propose a model for its formation and to discuss its possible functional significance.

Although Prezant (1981a) regarded the granular structure as being composed of spherules, our results reveal that they are actually prisms, albeit very short ones, composed of

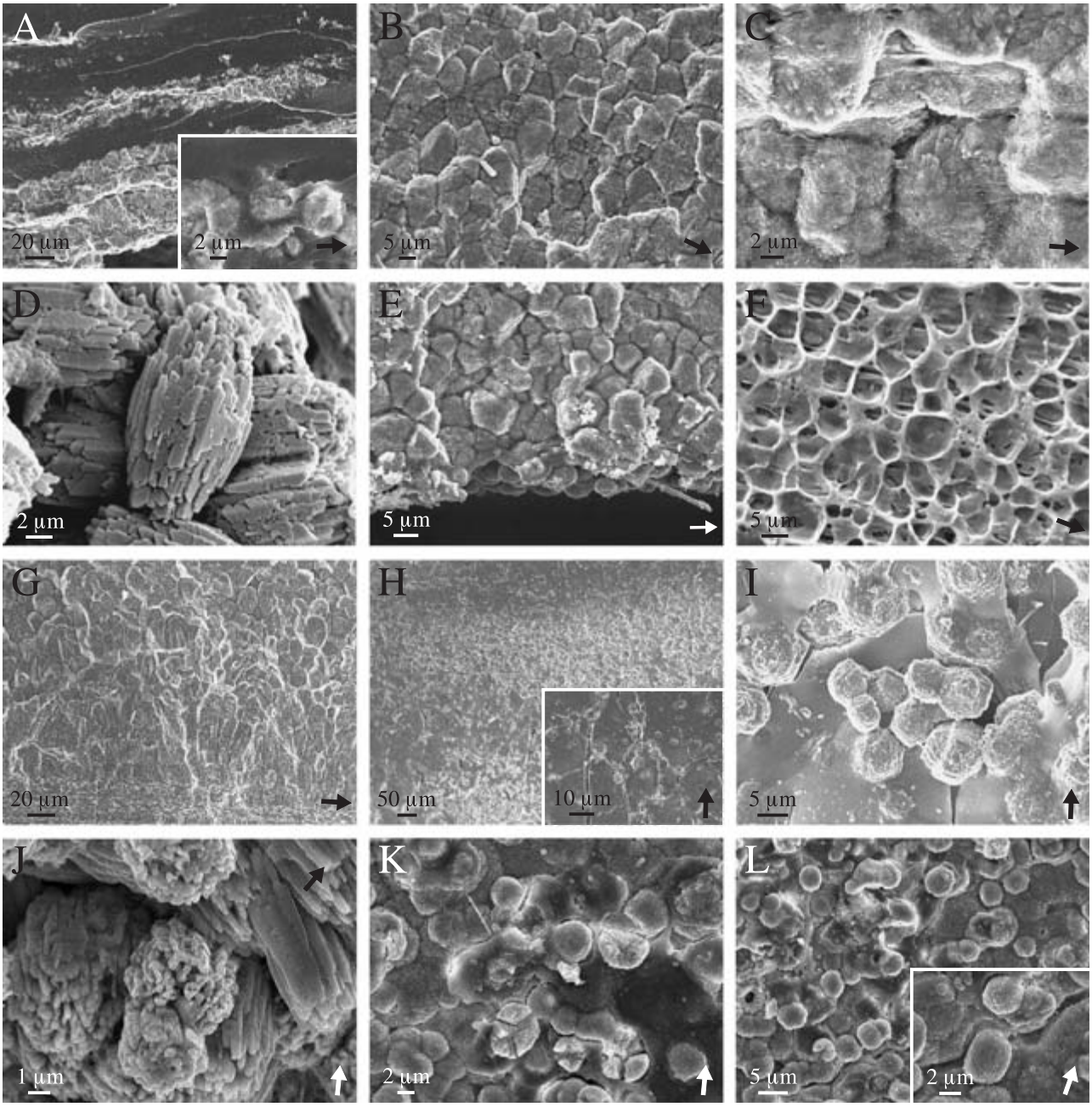

Fig. 4—Scanning electron micrographs of the 'homogeneous' microstructural layer of *Entodesma navicula*. —**A**. Radial fracture through the boundary between periostracum and granular layer, showing the interdigitation between both materials; the inset is a close-up view of the very initiation of a granular layer, with grains interspersed within the internal periostracum. —**B**. Radial fracture through the granular layer showing internal growth banding. —**C**. Detail of a region similar to that shown in B; grains are completely surrounded by organic matter, except for some voids, where grains develop crystalline faces. —**D**. Detail of radial fracture through the granular layer in part which is more 'loosely packed'. —**E**. Radial fracture through the granular layer illustrating that the growth surface is irregular with protruding granules at very different growth stages. —**F**. Decalcified section of the granular layer; the growth bands are marked by parallel organic membranes going across different grains. —**G**. Radial fracture through the lower portion of the granular layer and the initiation of the nacre layer; close to the boundary, grains elongate and acquire a pseudoprismatic aspect (compare to Fig. 3F). —**H**. Surface view of the granular layer; there are bands that are relatively richer in grains (bright areas) and in organic matter (darker areas); the inset corresponds to an area particularly rich in organic matter. —**I**. Close-up view of the surface of the granular layer showing the short prismatic (pseudohexagonal) aspect of grains embedded within organic layers; with exceptions, prisms tend to be arranged with their axes perpendicular to the growth surface. —**J**. Aggregation of slightly skeletal euhedral aragonite prisms, which were found in a void between periostracum and the granular layer; the cross-sections of fibres have a three-rayed arrangement indicative of the polycyclic {110} aragonite twinning. —**K.** Growth surface of the granular layer, with slightly pseudohexagonal grains embedded in organic matter; the main trend is for the grains to align with their axes perpendicular to the growth surface; note three-rayed fracture pattern of some grains. —**L**. As in K, with grains corresponding to very different growth stages; the inset shows very incipient grains (< 0.5 µm), together with others at an advanced stage of growth. Arrows indicate the growth direction of the margin.

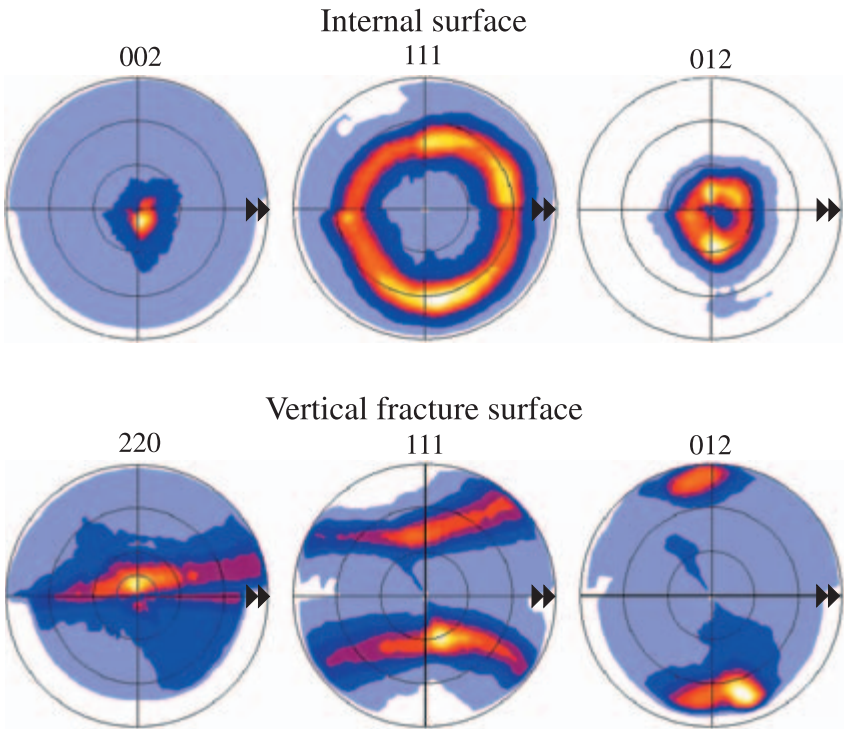

Fig. 5—Pole figures determined by X-ray diffraction texture analysis for the 'homogeneous' layer of *Entodesma*. Analyses have been made on both the outer (not shown) and inner surfaces and the fracture surface. The 002 pole figure displays a unique central maximum, implying that the crystals are orientated with their *c*-axes coaligned and perpendicular to the shell surface. Pole figures 111 and 102 for the internal surface as well as those three obtained on fracture surface (lower row) indicate that crystals have their *a*- and *b*-axes freely rotated around the *c*-axis (fibre texture, with the *c*-axis as fibre axis). The pole figures obtained on the external surface provide the same results. The growth direction of the shell (►►) is indicated.

crystals twinned along the {110} planes (as is typical for aragonite). The prismatic crystals are arranged in a fibrous texture where the *c*-axes and fibre axes are coincident, orientated perpendicular to the growth surface. It is therefore clear that this structure is not truly homogeneous.

Despite the identification of this microstructure as prismatic, it differs significantly from other types of prismatic microstructures found in molluscs. In particular, these prismatic crystals are distinct from the aragonitic prisms secreted by other bivalves (e.g. unionids, neotrigoniids). The more typical aragonite prisms are compact polycrystalline aggregations and have been classified by Ubukata (1994) as 'non-denticular composite prisms'. Because of these differences we propose the new term, 'granular prismatic' for the microstructure described herein.

Granular prisms also appear distinctive in their mode of growth. Previous observations (Nakahara and Bevelander 1971; Checa 2000; Checa and Rodríguez-Navarro 2005) have shown that growth of bivalve shells normally takes place on a very regular surface with crystals nucleating on the inner surface of the periostracum (and subsequent shell layers) and growing in intimate association with the outer face of the mantle into a thin extra-pallial, fluid-filled space. In these typical cases adjacent crystals are of similar size and growth lines within them truncate the crystals such that the inner growing surface of the shell is relatively smooth even at microscopic level. By contrast, in the case of granular prismatic microstructure the growth surface is uneven, with adjacent crystals at different stages of growth and embedded in a high proportion of organic material. It is clear that their growth is not limited to this surface but also occurs within a thick layer of gel, some distance away from the direct influence of the mantle. These differences require a modification of the mode of secretion other than that which is invoked for other microstructures, and for which we propose the model suggested below and summarized in Fig. 6.

Proposed model for the secretion of granular prisms

The uneven nature of the growth surface, with crystals growing simultaneously at different levels within the shell layer and the lack of truncated crystals at the growth surface suggests to us that the granular prismatic layer does not grow in direct contact with the mantle lobe. Instead we propose that the crystals nucleate in a substantial space 'above' the mantle (Fig. 6A). The thick rims and accumulations of organic material between the crystals suggest that this space is filled with a gel-like substance that becomes trapped between the growing crystals. There is no significant discontinuity between this gel-like substance and the inner periostracum, including the layers observed within them. Growth lines within the crystals cannot mark the position of the mantle because it is clear that not all adjacent grains reach this surface (Fig. 4E). We believe that the observed growth lines correspond to the initial layering of the periostracum and were produced as crystals grew in this gel across the layers. Crystals initiated within the gel continue to grow until they impinge on adjacent growing crystals, thereby trapping a thin rim of gel between them (Fig. 6A, right diagrams). Low diffusion rates of ions within a viscous gel may promote the

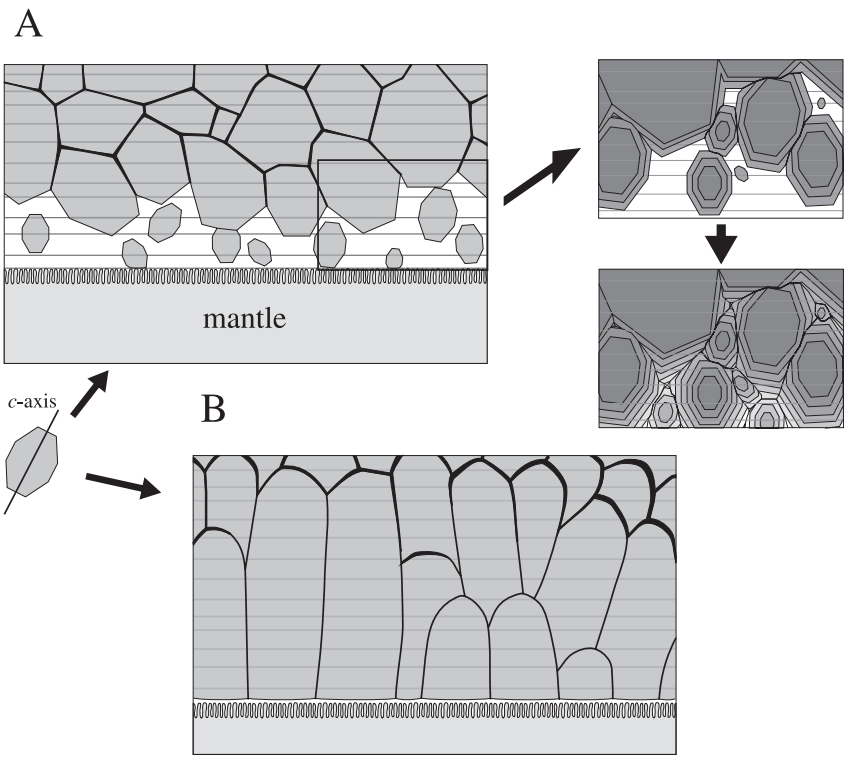

Fig. 6—Proposed model for the formation of granular prismatic microstructure of *Entodesma navicula*. —**A**. Growth of grains within the granular layer; the diagrams on the right shows how prismatic units transform into polyhedral grains when impingement is complete. —**B**. Situation close to the nacre, with grains transforming into elongate pseudoprismatic units. See text for detailed explanation.

anhedral nature of the crystals and their close contact prevents the development of crystalline faces. In certain situations, where more skeletal crystals form with well-defined faces (Fig. 4D,J), we suggest that the organic gel appears to be lacking, indicating that these crystals have grown in a low viscosity fluid (i.e. more like the typical extra-pallial fluid).

Although the granular prismatic microstructure appears disordered, X-ray diffraction analysis reveals that crystals are, in fact, mostly ordered with their *c*-axes perpendicular to the growth surfaces. Although such order in other prismatic microstructures is thought to result from competition of adjacent prisms growing from a common surface, this cannot be true in this case because the crystals are growing isolated and simultaneously at different levels within the gel-filled space. In this case, the presence of organic sheets parallel with the growth surface (Fig. 3B–F) may provide sites for orientated nucleation. We suggest that the ionotropic effect, as reported by Addadi *et al.* (1987), whereby the accumulation of charged ions on the surface of the organic sheets favours the orientated nucleation of aragonite (or calcite) with the positively charged calcium layers ({001} basal planes) parallel to the sheets, applies here.

As the shell thickens, however, conditions change. Just before the switch to the secretion of nacre, the character of the granular prisms changes as they become longer and more typical of columnar prisms seen elsewhere (Figs 3A and 4G). We suggest that this change is effected by the reduction of the gel-filled space and a closer involvement of the mantle. In these instances the crystals appear to have a common growth front suggesting that the space available for new crystals to nucleate is limited (Fig. 6B). There remain, however, basic differences between this pseudo-prismatic layer formed at the base of the homogeneous layer and the traditionally recognized aragonitic prismatic layer, typical of for example, unionids, where prisms originate as spherulites and are polycrystalline aggregates instead of the twinned prisms seen herein.

Evolution and significance of the structure

The typical anomalodesmatan shell microstructure comprises a thin external prismatic layer of aragonite and this arrangement is evident in other members of the Lyonsiidae, including some species of *Entodesma* (e.g. *E. pictum*, *E. beana*, *E. fretalis*, *E. patagonica* and *E. chilensis*) where it reaches thicknesses of around 10 μm. We envisage that in certain species of *Entodesma* the distinctive granular prismatic layer may be derived relatively easily from this primitive arrangement by simply increasing the relative distance between the mantle and the growing shell (Fig. 6). As noted by Prezant (1981a) these species are those, such as *E. navicula*, *E. cuneata* and *E. truncatissima*, that have with thicker shells and that tend to live intertidally between rocks. It is as yet unknown whether these taxa form a monophyletic group (as implied by the use of the subgenus *Agriodesma* for the

thicker-shelled species), united by possession of this microstructure, or whether it has arisen polyphyletically in closely related taxa experiencing similar environmental conditions. Nevertheless the evolution of this derived microstructure raises interesting questions as to the selection pressures involved.

One of the striking features of the granular prismatic microstructure of *Entodesma* is its very high organic content. Our figure of 7.4% is significantly greater than the range determined for other molluscan microstructures of 0.1–5.4% (Hare and Abelson 1964; Taylor and Layman 1972; Checa *et al.* 2005). There are a number of consequences and implications of this high organic content both in terms of the 'cost' of shell secretion and the mechanical properties of the shell.

Although the energetic costs involved in molluscan shell secretion are imperfectly known, it has been demonstrated that those microstructures with higher organic content are the most expensive to produce and maintain (Palmer 1983, 1992). If this is so, then far from being a cheap, easily acquired shell structure, as suggested by Prezant (1981a), granular prismatic microstructure is actually the most expensive yet known. It is therefore tempting to suggest that there must be some other selective benefit to the evolution of granular prismatic shell layers that appears to operate in the predominantly high energy intertidal habitats used by the thicker shelled species of *Entodesma.*

Unfortunately, we have been unable to obtain suitable fresh material to make a detailed study of the physical properties of the shells of *E. navicula* Although the mechanical and dissolution characteristics of a range of shell microstructures are available in the literature (Taylor and Layman 1972; Currey and Taylor 1974; Currey 1976; Gabriel 1981; Harper 2000), all studies have used *A. islandica* as the example of homogeneous microstructures simply because it is the most readily available taxon to provide material of the necessary dimensions for mechanical testing. Given the entirely different characteristics of the structure in *A. islandica*, not least its extremely low organic content, these data are entirely inappropriate for speculating on the behaviour of the shell of *E. navicula.*

One characteristic commonly associated with high organic content in molluscan shell material is flexibility (Taylor and Layman 1972; Checa *et al.* 2005). Although the specimens of *Entodesma* found in museum collections are often very fragile and break easily, this weakness is unlikely to afflict live material; there is good evidence that other highly organic microstructures become brittle after death and drying out (e.g. Yonge 1953). We have evidence that the shells of *E. navicula* are indeed flexible at their edges because our material, which had been fixed live and remained with both valves tightly adducted, show that the valve edges are flexed 'outwards' in such a position that it is clear that in conjoined valves they would have met and lain parallel to one another forming a flexible flange (Fig. 7). In this way they would have had valve margins similar to those of pinnoids and pterioid bivalves (see Yonge 1953; Harper and Morton 1994). We note that in museum specimens that have remained reasonably intact and articulated there is a tendency to exhibit a marked posterior gape. This, again, appears to be a post-mortem feature because the animal does not possess the long siphons which require a gape in life, and which must result from loss of flexibility in this region. This type of valve closure is often associated with the ability to form a tight hermetic seal against either the environment or would-be predators (Vermeij 1987). The effect of this would be further enhanced by periostracum, which overlaps the valve edge by a considerable degree. We propose that species of *Entodesma* living in the difficult intertidal zone gain adaptive advantage by the possession of a microstructure that allows them to develop a flexible tight seal thereby protecting them from desiccation.

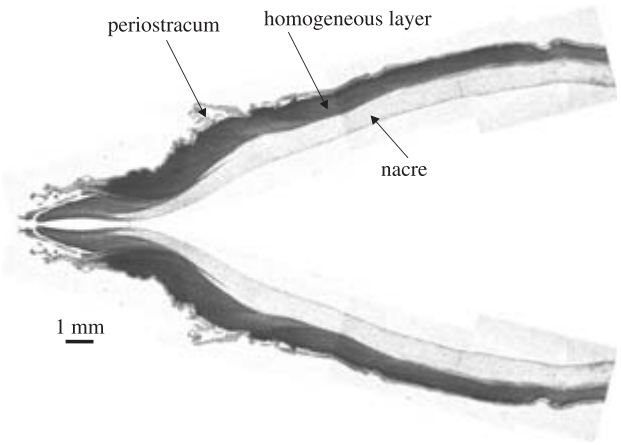

Fig. 7—Thin section through one valve of *Entodesma navicula* juxtaposed with its mirror image to demonstrate the flexible flange around the ventral margins.

Acknowledgements

We are grateful to Roland Anderson for the supply of material of *E. navicula* and also to Rüdiger Bieler, John Taylor and Paul Valentich-Scott for providing comparative material of other lyonsiids. Paul Valentich-Scott and Gene Coan are thanked for untangling the taxonomy of *E. navicula.* Research Projects CGL2004-00802 and CGL2007-60549 (DGI, MEC) and Research Group RNM190 (PAI, JA). This is Cambridge Earth Sciences Publication 9217.

References

Addadi, L., Moradian, J., Shay, E., Maroudas, N. G. and Weiner, S. 1987. A chemical model for the cooperation of sulfates and carboxylates in calcite crystals formation. – *Proceedings of the National Academy of Sciences, USA* **84**: 2732–2736.

Atlan, G., Balmain, N., Berland, S., Vidal, B. and Lopez, E. 1997. Reconstruction of human maxillary defects with nacre powder: histological evidence for bone regeneration. – *Comptes Rendus de l'Academie Des Sciences Serie III – Sciences de la Vie* **320**: 253–258.

Bøggild, O. B. 1930. The shell structure of mollusks. – *Det Kongelige Danske Videnskabernes Selskabs, Skrifter. Naturvidenskabelig Og Mathematisk Afdeling* **9**: 233–326.

Camprase, S., Camprase, G., Pouzol, M. and Lopez, E. 1990. Artificial dental root made of natural calcium carbonate (Bioracine). – *Clinical Materials* **5**: 235–250.

Carpenter, W. B. 1847. Report on the microscopic structure of shells. Part II. – *Report of the British Association for the Advancement of Science, 17th Meeting* **1847**: 93–134.

Carter, J. G. 1980. Environmental and biological controls of bivalve shell mineralogy and microstructure. In Rhoads, D. C. and Lutz, R. A. (Eds): *Skeletal Growth of Aquatic Organisms*, pp. 69–113. Plenum Press, New York and London.

Carter, J. G. and Clark, G. R. 1985. Classification and phylogenetic significance of Molluscan shell microstructure. In Broadhead, T. W. (Ed.): *Mollusks. Notes for a Short Course*, pp. 50–71. University of Tennessee Department of Geological Sciences Studies in Geology, Knoxville TN.

Checa, A. G. 2000. A new model for periostracum and shell formation in Unionidae (Bivalvia, Mollusca). – *Tissue and Cell* **32**: 405–416.

Checa, A. G. and Rodríguez-Navarro, A. 2001. Geometrical and crystallographic constraints determine the self-organization of shell microstructures in Unionidae (Bivalvia: Mollusca). – *Proceedings of the Royal Society of London B* **268**: 771–778.

Checa, A. G. and Rodríguez-Navarro, A. B. 2005. Self-organisation of nacre in the shells of Pterioida (Bivalvia: Mollusca). – *Biomaterials* **26**: 1071–1079.

Checa, A. G., Rodríguez-Navarro, A. and Esteban-Delgado, F. J. 2005. The nature and formation of calcitic columnar prismatic shell layers in pteriomorphian bivalves. – *Biomaterials* **26**: 6404–6414.

Coan, E. V., Valentich Scott, P. and Bernard, F. R. 2000. *Bivalve Seashells of Western North America*. Santa Barbara Museum of Natural History, Santa Barbara.

Currey, J. 1970. D: The mechanical properties of bone. – *Clinical Orthopaedics* **73**: 210–231.

Currey, J. D. 1976. Further studies on the mechanical properties of mollusc shell material. – *Journal of Zoology, London* **180**: 445–453.

Currey, J. D. and Taylor, J. D. 1974. The mechanical behavior of some molluscan hard tissues. – *Journal of Zoology, London* **173**: 395–406.

Dreyer, H., Steiner, G. and Harper, E. M. 2003. Molecular phylogeny of Anomalodesmata (Mollusca: Bivalvia) inferred from 18S rRNA sequences. – *Zoological Journal of the Linnean Society* **139**: 229–246.

Gabriel, J. M. 1981. Differing resistance of various mollusc shell material to simulated whelk attack. – *Journal of Zoology, London* **194**: 363–369.

Hare, P. E. and Abelson, P. H. 1964. Proteins in mollusk shells. – *Report of the Director, Geophysics Laboratory, Carnegie Institution, Washington* **63**: 267–270.

Harper, E.M. 2000. Are calcitic layers an effective adaptation against shell dissolution in the Bivalvia? – *Journal of Zoology* **251**: 179–186.

Harper, E. M., Dreyer, H. and Steiner, G. 2006. Reconstructing the Anomalodesmata (Mollusca: Bivalvia): morphology and molecules. – *Zoological Journal of the Linnean Society* **148**: 395–420.

Harper, E. and Morton, B. 1994. The biology of *Isognomon legumen* (Gmelin, 1791) (Bivalvia: Pterioida) at Cape d'Aguilar, Hong Kong, with special reference to predation by muricids. In Morton, B. (Ed.): *The Malacofauna of Hong Kong and Southern China III*, pp. 402–425. Hong Kong University Press, Hong Kong.

Lin, A.Y., Chen, P.Y. and Meyers, A. 2008. The growth of nacre in the abalone shell. – *Acta Biomateralia* **4**: 131–138.

Morgan, R. E. and Allen, J. A. 1976. On the functional morphology and adaptations of *Entodesma saxicola* (Bivalvia: Anomalodesmacea). – *Malacologia* **15**: 233–240.

Morris, R. H., Abbott, D. P. and Haderlie, E. C. 1980. *Intertidal Invertebrates of California*. .Stanford University Press, Stanford, CA.

Morton, B. 1987. The mantle margin and radial mantle glands of *Entodesma saxicola* and *E. inflata* (Bivalvia: Anomalodesmata: Lyonsiidae). – *Journal of Molluscan Studies* **53**: 139–151.

Nakahara, H. and Bevelander, G. 1971. The formation and growth of the prismatic layer of *Pinctada radiata*. – *Calcified Tissue Research* **7**: 31–45.

Oberling, J. J. 1964. Observations on some structural features of the pelecypod shell. – *Mitteilungen der Naturforschenden Gessellschaft in Bern* **20**: 1–63.

Palmer, A. R. 1983. Relative cost of producing skeletal organic matrix versus calcification: evidence from marine gastropods. – *Marine Biology* **57**: 287–292.

Palmer, A. R. 1992. Calcification in marine molluscs: how costly is it? – *Proceedings of the National Academy of Sciences, USA* **89**: 1379–1382.

Prezant, R. S. 1981a. Comparative shell ultrastructure of lyonsiid bivalves. – *Veliger* **23**: 289–299.

Prezant, R. S. 1981b. Taxonomic re-evaluation of the bivalve family Lyonsiidae. – *Nautilus* **95**: 58–72.

Prezant, R. S. 1981c. The arenophilic radial mantle glands of the Lyonsiidae (Bivalvia: Anomalodesmata) with notes on lyonsiid evolution. – *Malacologia* **20**: 267–289.

Rodríguez-Navarro, A. B. 2007. Registering pole figures using an X-ray single-crystal diffractometer equipped with an area detector. – *Journal of Applied Crystallography* **40**: 631–634.

Ropes, J. W., Jones, D. S., Murawski, S. A., Serchuk, F. M. and Jearld, A. 1983. Documentation of annual growth lines in Ocean Quahogs, *Arctica islandica* Linné. – *Fishery Bulletin* **82**: 1–19.

Taylor, J. D. 1973. The structural evolution of the bivalve shell. – *Palaeontology*. **16**: 519–534.

Taylor, J. D., Kennedy, W. J. and Hall, A. D. 1969. The shell structure and mineralogy of the Bivalvia. Introduction, Nuculacea-Trigonacea. – *Bulletin of the British Museum (Natural History), Zoology Seriessupplement* **3**: 1–125.

Taylor, J. D., Kennedy, W. J. and Hall, A. D. 1973. The shell structure and mineralogy of the Bivalvia. II. Lucinacea-Clavagellacea, Conclusions. – *Bulletin of the British Museum (Natural History), Zoology Series* **22**: 225–294.

Taylor, J. D. and Layman, M. 1972. The mechanical properties of bivalve (Mollusca) shell structures. – *Palaeontology* **15**: 73–87.

Ubukata, T. 1994. Architectural constraints on the morphogenesis of prismatic structure in Bivalvia. – *Palaeontology* **37**: 241–261.

Vermeij, G. J. 1987. *Evolution and Escalation. An Ecological History of Life*. Princeton University Press, Princeton, NJ.

Yonge, C. M. 1952. Structure and adaptation in *Entodesma saxicola* (Baird) and *Mytilimeria nuttallii* Conrad. – *University Of California Publications in Zoölogy* **55**: 439–450.

Yonge, C. M. 1953. Form and habit in *Pinna carnea* Gmelin. – *Philosophical Transactions of the Royal Society* **237**: 335–374.